Phospholipid homeostasis regulates lipid metabolism and cardiac function through SREBP signaling in *Drosophila*

Hui-Ying Lim,[1] Weidong Wang,[2] Robert J. Wessells,[3] Karen Ocorr,[1] and Rolf Bodmer[1,4]

[1]Development and Aging Program, NASCR (Neuroscience, Aging, and Stem Cell Research) Center, Sanford-Burnham Medical Research Institute, La Jolla, California 92037, USA; [2]The Skaggs Institute of Chemical Biology, The Scripps Research Institute, La Jolla, California 92037, USA; [3]Department of Internal Medicine, Institute of Gerontology, University of Michigan Medical School, Ann Arbor, Michigan 48109, USA

The epidemic of obesity and diabetes is causing an increased incidence of dyslipidemia-related heart failure. While the primary etiology of lipotoxic cardiomyopathy is an elevation of lipid levels resulting from an imbalance in energy availability and expenditure, increasing evidence suggests a relationship between dysregulation of membrane phospholipid homeostasis and lipid-induced cardiomyopathy. In the present study, we report that the *Drosophila easily shocked* (*eas*) mutants that harbor a disturbance in phosphatidylethanolamine (PE) synthesis display tachycardia and defects in cardiac relaxation and are prone to developing cardiac arrest and fibrillation under stress. The *eas* mutant hearts exhibit elevated concentrations of triglycerides, suggestive of a metabolic, diabetic-like heart phenotype. Moreover, the low PE levels in *eas* flies mimic the effects of cholesterol deficiency in vertebrates by stimulating the *Drosophila* sterol regulatory element-binding protein (dSREBP) pathway. Significantly, cardiac-specific elevation of dSREBP signaling adversely affects heart function, reflecting the cardiac *eas* phenotype, whereas suppressing dSREBP or lipogenic target gene function in *eas* hearts rescues the cardiac hyperlipidemia and heart function disorders. These findings suggest that dysregulated phospholipid signaling that alters SREBP activity contributes to the progression of impaired heart function in flies and identifies a potential link to lipotoxic cardiac diseases in humans.

[*Keywords*: phospholipid homeostasis; SREBP; lipid metabolism; cardiac function; lipotoxic cardiomyopathy]

Supplemental material is available for this article.

Received September 13, 2010; revised version accepted December 8, 2010.

Obesity has reached global epidemic proportions in both adults and children and is associated with significant morbidity and mortality. Obesity and other factors such as diabetes, hypertension, and hyperlipidemia constitute a constellation of factors known as the metabolic syndrome that are known risk factors for coronary artery disease, which is the most common cause of heart failure in the United States (Schulze 2009). While it is well known that the metabolic syndrome contributes to atherosclerotic vascular diseases, emerging evidence suggests that it can also directly impact cardiac function independently of cardiovascular artherosclerosis. Under conditions of obesity and diabetes, dyslipidemia could lead to inappropriate accumulation of lipids in peripheral tissues such as the myocardium, resulting in organ malfunction, a process termed lipotoxicity. Various approaches have been undertaken to characterize the fundamental mechanisms underlying cardiac lipotoxicity in rodent models of obesity and diabetes and in transgenic mice with lipotoxic cardiomyopathy (Chiu et al. 2001, 2005; Christoffersen et al. 2003; Yagyu et al. 2003; Son et al. 2007). These studies have helped in the understanding of how a mismatch between fatty acid and glucose uptake and use may result in increased deposition of free fatty acids and neutral lipids within the cardiomyocytes. This lipid overload could elicit the generation of detrimental lipotoxic metabolites that in turn induce cardiac dysfunction by multiple mechanisms, including the alteration of cellular signaling (Yang and Barouch 2007), mitochondria dysfunction (Bugger and Abel 2008), and lipoapoptosis (Unger and Orci 2002).

While many studies on lipotoxicity in the heart focused on the pathogenesis of cardiomyopathy associated with lipid surpluses in lipid storage diseases such as obesity, an intriguing hypothesis for an alternative cause of lipotoxicity that has not been explored in detail in the heart is the relationship between altered membrane phospholipid homeostasis and lipid-induced cardiac dysfunction. A

[4]Corresponding author.
E-MAIL rolf@burnham.org; FAX (858) 795-5298.
Article is online at http://www.genesdev.org/cgi/doi/10.1101/gad.1992411.

growing body of evidence is revealing the significance of impaired phospholipid-mediated signaling systems in cardiac hypertrophy, diabetic cardiomyopathy, and heart failure (Tappia and Singal 2008), all of which could be associated with excessive cardiac lipid accumulation. In vitro studies have also supported this notion of an association between dysregulated phospholipid metabolism and cardiac lipotoxicity. For instance, a decreased synthesis of the signature mitochondrial membrane phospholipid cardiolipin corresponds with cytochrome c release in palmitate-induced cardiomyocyte apoptosis (Ostrander et al. 2001). Moreover, free fatty acid overloading of cultured rat myocytes elicited phospholipid breakdown and culminated in cell death (Janero et al. 1988). Last, but not least, it was found that a major cardioprotective effect of trimetazidine in rats was due to an increased synthesis of membrane phospholipids, which may direct a rebalancing of fatty acid use in the heart (Sentex et al. 1997, 1998). It was further proposed that the preservation of membrane phospholipid homeostasis could be considered as a therapeutic target in the treatment of heart failure (Tabbi-Anneni et al. 2003). Clearly, it is important to investigate the functional roles of cellular phospholipids in cardiac steatosis and malfunction, and this would require the characterization of upstream mechanisms regulating the metabolism of phospholipids as well as the downstream phospholipid-mediated signaling events.

Phosphatidylethanolamine (PE) is the second most abundant phospholipid in mammals (Leonardi et al. 2009) and the major phospholipid in most dipterans (Fast 1966). The CDP–ethanolamine pathway is the principal route for PE synthesis in most mammalian tissues, with the first step requiring ethanolamine kinase (McMaster and Choy 1992). In *Drosophila*, the *easily shocked* (*eas*)-encoded ethanolamine kinase catalyzes the phosphorylation of ethanolamine to phosphoethanolamine (Fig. 1I; Kennedy 1957). Phosphoethanolamine is further modified by phosphoethanolamine cytidylytransferase (PECT) to produce CDP–ethanolamine, which, together with diacylglycerol (DAG), generates PE (Fig. 1I; Dobrosotskaya et al. 2002). Consistent with its role in this pathway, the activity-null mutant of *eas* (eas^2) (Pavlidis et al. 1994) shows virtually no detectable ethanolamine kinase activity throughout development and exhibits a decrease in the level of PE (Pavlidis et al. 1994; Nyako et al. 2001).

PE and its downstream signaling events appear to play a significant role in proper functioning of the heart, as seen by an alteration in the asymmetrical transbilayer distribution of PE in sarcolemmal membranes during

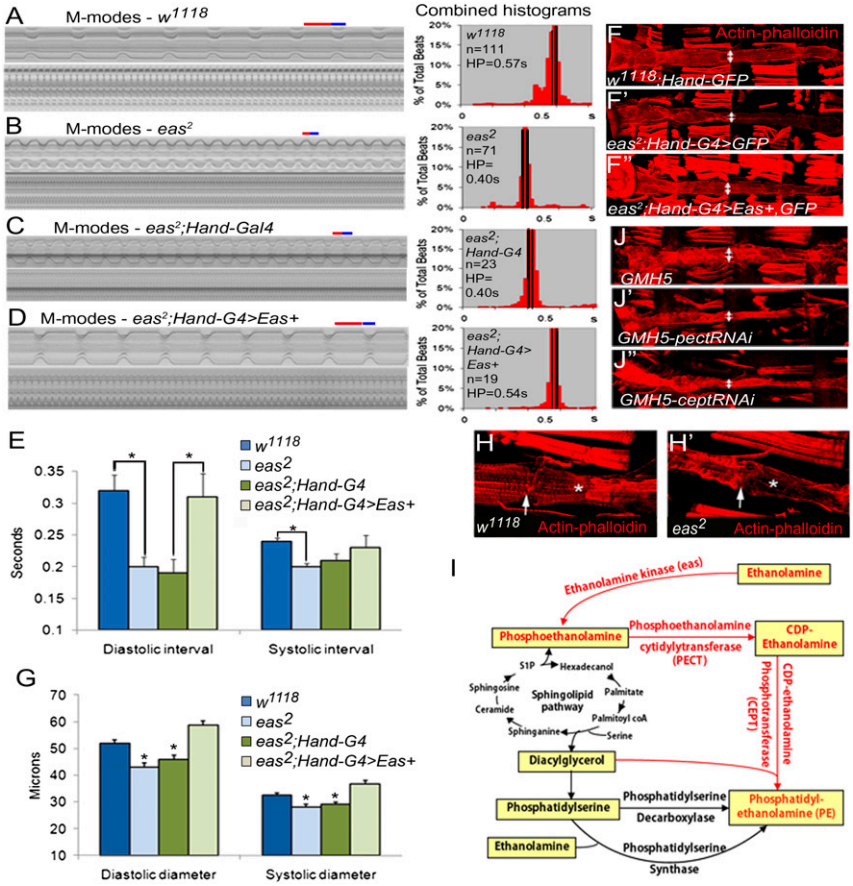

Figure 1. The *eas* fly exhibits defects in cardiac physiology. (*A–D*) Representative M-mode traces (5 and 30 sec) showing movement of heart tube walls (*Y*-axis) over time (*X*-axis). Histograms indicate the distribution of HP for all flies normalized to the average of the median values (Fink et al. 2009). Diastolic (red) and systolic (blue) intervals were indicated *above* each M-mode trace. *n* = number of female adult hearts. HP in *A* and *B* represents pooled 1- and 3-wk-old data; HP in *C* and *D* represents 3-wk-old data. (*E*,*G*) Bar graph representations of changes in HPs and heart chamber dimensions. *P*-values ([*] $P < 0.05$) were calculated using the Student's *t*-test. Error bars indicate SEM. Values for w^{1118} and eas^2 represent pooled 1- and 3-wk-old data; values for others represent 3-wk-old data. (*F*,*H*,*J*) Representative confocal images of adult female hearts (anterior to left) stained with actin-phalloidin (red). Arrows indicate similar regions of the cardiac vessel. (*F–F″*) The constricted heart tube in eas^2 (*F′*) is restored to wild-type size (*F*) by cardiac-targeted expression of Eas^+ (*F″*). (*H*) The eas^2 hearts exhibit significant loss and misarrangement of longitudinal and transverse myofibers (astericks). (*I*) Schematic overview of the various pathways of PE biosynthesis in eukaryotic cells. The scheme is modified from Dobrosotskaya et al. (2002). Reprinted with permission from AAAS. Note that, in addition to the CDP–ethanolamine pathway (red), sphingolipids and other phospholipids such as phosphatidylserine can also feed into PE synthesis. Thus, *eas* deficiency only partially reduces PE levels. (*J–J″*) Hearts expressing RNAi constructs of pect and cept are considerably thinner than the control hearts.

ischemia, leading to sarcolemmal disruption (Post et al. 1995). Moreover, abnormalities were found in the molecular species profile of PE that could contribute to membrane dysfunction and defective contractility of the diabetic heart (Vecchini et al. 2000). Whereas many individual phospholipid constituents are known to be involved in specific signaling functions necessary for cells to respond to external stimuli, the specific signaling function of PE is largely unknown (Yao et al. 2009). From *Drosophila* tissue culture studies, it was postulated that PE could regulate the processing and hence signaling activity of the *Drosophila* sterol regulatory element-binding protein (dSREBP) (Dobrosotskaya et al. 2002). The SREBPs comprise a subfamily of basic helix–loop–helix leucine zipper transcription factors that are conserved global regulators of lipid homeostasis (Osborne and Espenshade 2009). In response to various external stimuli, the precursor SREBP proteins are transported from the endoplasmic reticular (ER) membrane to the Golgi by the SCAP-Insig escort proteins, where they undergo proteolytic processing to release the transcriptional active domain, which translocates to the nucleus to induce cholesterol/lipogenic gene expression. Consistent with their critical roles in lipid synthesis, the aberrant activation of SREBPs could contribute to obesity-related pathophysiology in various organs, including cardiac arrhythmogenesis and hepatic insulin resistance (Shimano 2009).

In the present study, we explore the genetic–molecular links between dysregulated phospholipid metabolism and lipotoxic cardiomyopathy in the *Drosophila eas*^{2} model. We discovered severe abnormalities in the cardiac physiology of adult *eas*^{2} flies, with their hearts beating faster and exhibiting severe constriction akin to restrictive cardiomyopathy in humans. Under acute stress, the *eas*^{2} mutant hearts succumb more frequently to arrest and fibrillation. These abnormalities are attributed to increased lipogenesis and triglyceride accumulation in the heart. The elevation in lipid concentrations in the *eas*^{2} fly is caused by abnormal activation of the dSREBP pathway, most likely as a compensatory hyperactive response to constitutive deficiency in PE levels. Genetic manipulations to reduce the expression or activity of dSREBP in the *eas*^{2} whole fly or heart lead to the rescue of the cardiac and lipid derangements. This study provides novel insight into the genetic relationship between phospholipid homeostasis and lipotoxic cardiomyopathy through the regulation of SREBP activity. The cardiac-autonomous role of SREBP in modulating heart function also identifies this component of phospholipid signaling as a candidate target for future therapies aimed at obesity- and diabetes-related cardiac dysfunction.

Results

eas mutant flies exhibit defects in cardiac physiology

To identify candidate genes for cardiac function and aging, a heart performance screen in response to external electrical pacing (Wessells et al. 2004) was conducted using a random collection of *Drosophila* P-insertion lines, leading to the identification of *eas* as a candidate modulator of adult heart function (data not shown). We then examined the cardiac physiology of the activity-null fly mutant of *eas* (*eas*^{2}) using image-based assessment of heart function that combines high-speed optical recording of semi-intact adult preparations of beating (denervated) hearts with semiautomated analysis software for the quantification of heart function parameters (K Ocorr et al. 2007b; Fink et al. 2009). The video-captured M-modes of hearts revealed a significant reduction in the average heartbeat length (heart period [HP]) (see combined histograms in Fig. 1A,B; Supplemental Tables S1, S2) of *eas*^{2} as compared with wild-type (*w*^{1118}) (see the Materials and Methods). The shortened HP of *eas*^{2} flies is due to decreased diastolic and systolic intervals (Fig. 1A,B,E, red and blue lines above M-modes). Additionally, the *eas*^{2} hearts are more constricted than wild-type hearts, as measured in live (Fig. 1G) or fixed preparations (Fig. 1F–F″). Because diastolic and systolic diameters seem to be reduced proportionally, *eas*^{2} hearts do not show a change in fractional shortening, but the absolute volume output of the *eas* heart is dramatically reduced (by ~40%) (data not shown). In addition, the regular ventral longitudinal myofibrils of the heart are considerably disrupted in *eas*^{2} hearts (Fig. 1H,H′). We further analyzed the heart contractile properties of *eas*^{KG01772}, a P-element insertion in *eas* that results in less *Eas*$^{+}$ protein being produced as compared with wild-type (Supplemental Fig. S1A). The transheterozygote of *eas*^{2} and *eas*^{KG01772} also generates an increased tendency to have a faster heart rate (Supplemental Fig. S2A–C) as well as a significantly constricted heart tube (Supplemental Fig. S2D), thereby partially phenocopying the *eas*^{2} mutant heart defect.

To determine if the cardiac abnormalities seen in the *eas*^{2} fly is specific to *eas*, we attempted to re-express a wild-type *Eas*$^{+}$ cDNA in the hearts of *eas*^{2} mutants using the cardiac-specific driver *Hand-Gal4* (Supplemental Fig. S1B). This significantly normalizes ("rescues") the reduced HP of the *eas*^{2} fly (Fig. 1B–D; Supplemental Table S1), mainly by restoring the diastolic interval to normal levels (Fig. 1E). In addition, the cardiac chamber also appears to regain normal size upon the overexpression of wild-type *Eas*$^{+}$ in the *eas*^{2} hearts (Fig. 1F–F″), with both the diastolic and systolic diameters evidently rescued to normal levels (Fig. 1G; Supplemental Table S1). Taken together, these results demonstrate that *EAS* function is critical for regulating normal heartbeat and contractility in a tissue-autonomous fashion.

Since *eas* encodes ethanolamine kinase involved in the biosynthesis of PE (Fig. 1I), we asked whether the associated cardiac defects were due to insufficient PE synthesis through the CDP–ethanolamine pathway. Compared with control hearts (Fig. 1J), the cardiac-specific expression of transgenic RNAi constructs against *pect* and *cept* both led to *eas*^{2}-like heart tube constriction (Fig. 1J′,J″; Supplemental Fig. S3C) and a trend toward a faster heart rate (Supplemental Fig. S3A,B; Supplemental Table S2), indicating that it is likely the cardiac dysregulation of PE metabolism that contributes to the *eas* heart derangements.

EAS function is required for proper heart performance under stress

In addition to its role in modulating cardiac physiology, *EAS* may also be involved in the maintenance of cardiac performance under conditions of acute stress, such as external electrical pacing-induced stress. In this stress test, heart performance is visually assessed by monitoring the incidence of cardiac arrest or fibrillation (termed "heart failure") (Wessells and Bodmer 2004). Adult heart response to pacing-induced stress is age-dependent and has been used as a measure of adult cardiac senescence (Wessells et al. 2004). Upon being subjected to pacing-induced stress, the eas^2 flies exhibited elevated incidences of heart failure at both young (1 and 2 wk) and old (4 wk) ages, with failure rates of young eas^2 mutant hearts being comparable with old wild-type hearts (Fig. 2A). Expression of wild-type Eas^+ cDNA in eas^2 hearts is sufficient to rescue the stress-induced heart failure rates of eas^2 hearts to normal levels (Fig. 2B), demonstrating that tissue-autonomous loss of *eas* may elicit precocious and augmented cardiac aging. Moreover, when overexpressing Eas^+ in wild-type hearts, we found that heart performance under stress was improved even at young ages (Fig. 2C), implying that gain of *EAS* function is cardioprotective under stress.

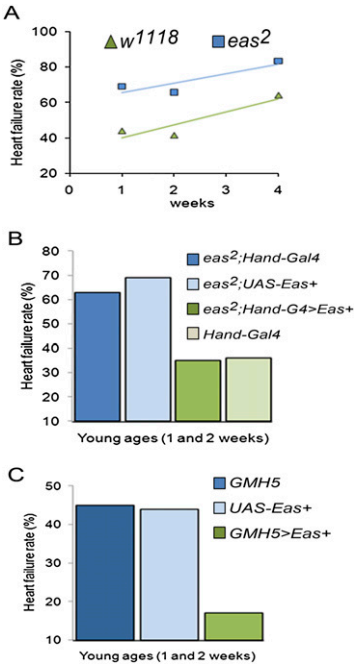

Figure 2. eas^2 is required in a tissue-autonomous manner for proper heart performance under stress. (*A*) Cardiac failure rates of adult flies at different ages in response to pacing-induced stress. The eas^2 flies (blue) exhibit a higher frequency of cardiac failure at all ages when compared with same-aged wild-type (w^{1118}) flies (green). The failure rates of eas^2 flies at 1 and 2 wk old are similar to that of w^{1118} flies at 4 wk old. About 60 flies were assayed per time point. (*B*) Cardiac failure rates in response to stress. Values represent pooled 1- and 2-wk-old failure rates. The high incidence of heart failure in eas^2 flies was rescued to normal levels (*Hand-Gal4*) upon cardiac expression of Eas^+. About 60 flies were assayed per genotype. (*C*) Cardiac failure rates in response to stress. The rates of heart failure in *GMH5*-overexpressing Eas^+ hearts (green) is less pronounced in comparison with the respective driver (blue bar) and transgene controls (light blue). About 60 flies were assayed per genotype.

Lipid metabolism is dysregulated upon perturbations in PE homeostasis

Several lines of evidence from tissue culture and murine studies have revealed a metabolic interconnection between the quantitatively most important phospholipids and triglycerides (TGs). Although phospholipids and TGs have different functions, these lipids are potentially subject to coregulation because they share common substrates and metabolic routes (Caviglia et al. 2004). Indeed, it was found that lipid intermediates released from phospholipids, such as DAG and fatty acids, can be used for TG synthesis (Vance 2008), and there is limited evidence that shows that the disruption of PE synthesis in mice could led to increased formation of TGs (Fullerton et al. 2009; Leonardi et al. 2009). This prompted us to investigate the possibility that similar changes in TG and fatty acid metabolism could occur in the eas^2 fly in response to decreased PE synthesis. We first measured TG levels in wild-type control (w^{1118}) and eas^2 mutant flies that were aged for 1 wk after eclosion, and found that the eas^2 mutants exhibit a dramatic increase in TG levels (by nearly 50%) compared with control flies (Fig. 3A). We also measured TG levels in eas^2 hearts and observed a similar elevation of TG levels over w^{1118} control hearts (by ~20%) (Fig. 3B), suggesting that the eas^2 fly exhibits cardiac steatosis. Importantly, the global knockdown of *pect* and *cept* by RNAi also led to an increase in TG levels compared with control flies (Fig. 3C), suggesting that hypertriglyceridemia in eas^2 is a consequence of defects in PE homeostasis.

Up-regulation of TG levels is generally associated with changes in fatty acid metabolism, with the three key enzymes that are required to divert glycolytic carbon flux into fatty acid biosynthesis being acetyl-coA carboxylase (ACC), ATP citrate lyase (ATPCL), and fatty acid synthase (FAS) (Shimano 2009). ATPCL converts cytosolic citrate into acetyl-CoA and oxaloacetate, thereby supplying the essential metabolite for lipid biosynthesis. Acetyl-CoA is in turn converted to malonyl-CoA by ACC before being used to generate long-chain fatty acids in a reaction catalyzed by FAS. We observed that the elevated TG levels in eas^2 flies and hearts are strongly suppressed upon reduced expression of genes encoding *ACC* and *FAS* by either the replacement of one functional copy of *ACC* with its mutant allele, ACC^{B131}, in the eas^2 background, or cardiac-specific RNAi knockdown of *FAS* (fas^{RNAi}) in the eas^2 mutant heart (Fig. 3A,B).

To further elucidate the potential roles of increased lipogenesis, increased uptake of fatty acids, or impaired degradation of lipids in contributing to hypertriglyceridemia in these flies, we examined the expression levels of ACC and ATPCL by Western blot analysis of whole-fly

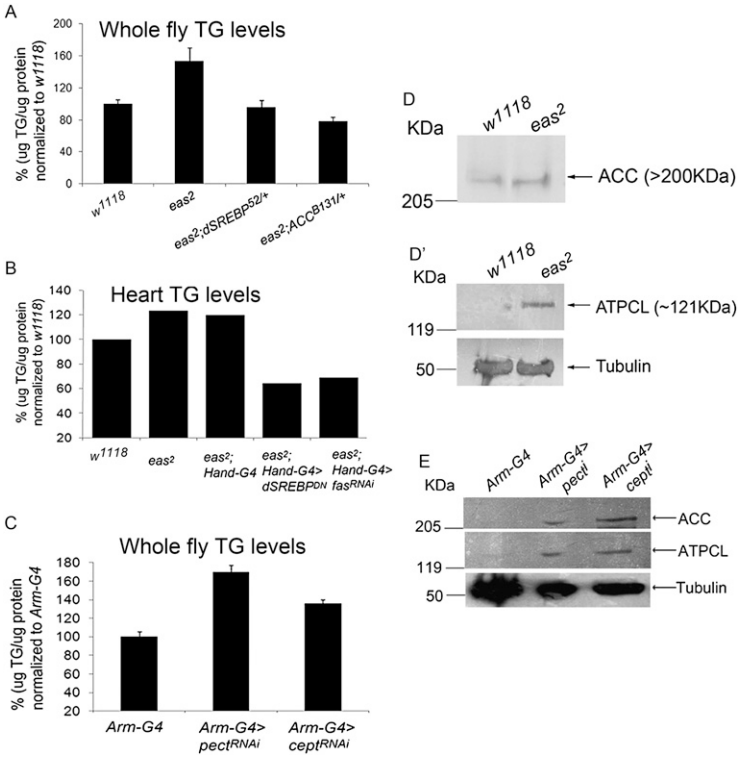

Figure 3. Lipid metabolism is dysregulated in whole flies and hearts harboring perturbations in PE homeostasis. (*A*) TG levels were detected using a colorimetric lipid oxidase assay in 1-wk-old female flies (20–24 flies total). TG levels were normalized for average weight per fly and are presented as normalized to a wild-type level of 100%. Three independent experiments were performed for each genotype. All error bars are ±SD. (*B*) TG levels are determined using a colorimetric lipid oxidase assay in 1-wk-old female hearts (~20 hearts total). TG levels were normalized for total protein and are presented as normalized to a wild-type level of 100%. Compared with wild-type hearts (w^{1118}), the eas^2 and outcrossed eas^2 whole flies and hearts exhibit increased amounts of TGs, which were suppressed upon global and heart-specific suppression of dSREBP signaling and fatty acid synthetic enzyme expression. (*C*) TG levels were detected using a colorimetric lipid oxidase assay in 1-wk-old female flies (10–14 flies total). TG levels were normalized for average weight per fly and are presented as normalized to a wild-type level of 100%. Three independent experiments were performed for each genotype. All error bars are ±SD. Compared with the driver control flies (*Arm-G4*), flies that overexpress the *RNAi* construct of *pect* (*Arm-G4>pectRNA*^{i}) or *cept* (*Arm-G4>ceptRNA*^{i}) exhibit increased amounts of TG levels. Protein expression of lipogenic enzymes ACC and ATPCL in 3-d-old female whole flies. (*D*,*D'*) Western blot analysis was carried out using a rabbit polyclonal antibody directed against human ACCα1 (Cell Signaling), which recognizes fly ACC (>280 kDa) (*D*), and a rabbit polyclonal antibody directed against human ATPCL (Cell Signaling), which recognizes fly ATPCL (~121 kDa) (*D'*). The total protein (~20 μg) for each lane was quantified by Bradford assay before loading. (*Bottom* panel) The same blot was probed with anti-tubulin antibody as a loading control. The eas^2 fly showed increased amounts of both ACC and ATPCL proteins relative to the wild-type fly. (*E*) Western blot analysis against ACC and ATPCL proteins were carried out using the above-described antibodies. Total protein (~10 μg) for each lane was quantified by Bradford assay before loading. (*Bottom* panel) The same blot was probed with anti-tubulin antibody as a loading control. Both ACC and ATPCL levels were elevated in flies overexpressing the *RNAi* construct of *pect* (*Arm-G4>pectRNA*^{i}) or *cept* (*Arm-G4>ceptRNA*^{i}) as compared with that in control flies (*Arm-G4*).

lysates. We observed enhanced expression levels of ACC and ATPCL in the eas^2 as well as global (*Arm-G4*-mediated) *pect* and *cept* knockdown ($pect^i$ and $cept^i$) flies relative to wild-type (w^{1118}) and control (*Arm-G4*) flies (Fig. 3D,E; see Supplemental Fig. S4 for ACC and ATPCL antibody specificity). These data indicate that a disruption of PE homeostasis in flies is associated with the stimulation of de novo lipogenesis, which facilitates the increased generation and accumulation of TG.

Altered lipid metabolism contributes to cardiac derangements in eas^2 flies

We next determined whether the increased production and accumulation of TGs may be responsible for the eas^2 heart disorders. To address this, we performed RNAi-mediated knockdown of lipogenic genes in either the heart or whole fly of eas^2 to ask whether they might alleviate cardiac disorders. The targeted expression of RNAi constructs against either *ATPCL* or *FAS* in the eas^2 hearts restored the heartbeat of the eas^2 fly (Fig. 4B,H) to normal (Fig. 4C,D,I,J). The constricted heart chamber phenotype in the eas^2 flies was also reversed to wild-type size in eas^2 flies with cardiac-targeted knockdown of *ATPCL* and *FAS* (Fig. 4M). Similar observations were made in eas^2 flies that also contain a heterozygous deletion of either *ACC* or *FAS* (Fig. 4E,F,K,L; Supplemental Fig. S5A). The diastolic and systolic diameters of these flies were significantly restored as well (Fig. 4N; Supplemental Fig. S5B). Taken together, these results indicate that reduced PE synthesis in the eas^2 fly stimulates fatty acid production and TG accumulation, which is accompanied by the development of cardiomyopathies that can be prevented by genetically counteracting lipid overloading.

Aberrant dSREBP signaling contributes to adiposity and cardiac deficits in eas^2 flies

Our data so far point toward an important interaction between PE and fatty acid/TG metabolism that seems to have a critical role in modulating adult heart function in flies. Although previous studies have demonstrated a link between PE homeostasis and TG metabolism that could play a significant role in the development of fatty liver and insulin resistance (Fullerton et al. 2009; Leonardi et al. 2009), the specific signaling and transcriptional pathway involved in mediating dyslipidemia and disease pathogenesis in response to deficient PE levels was not

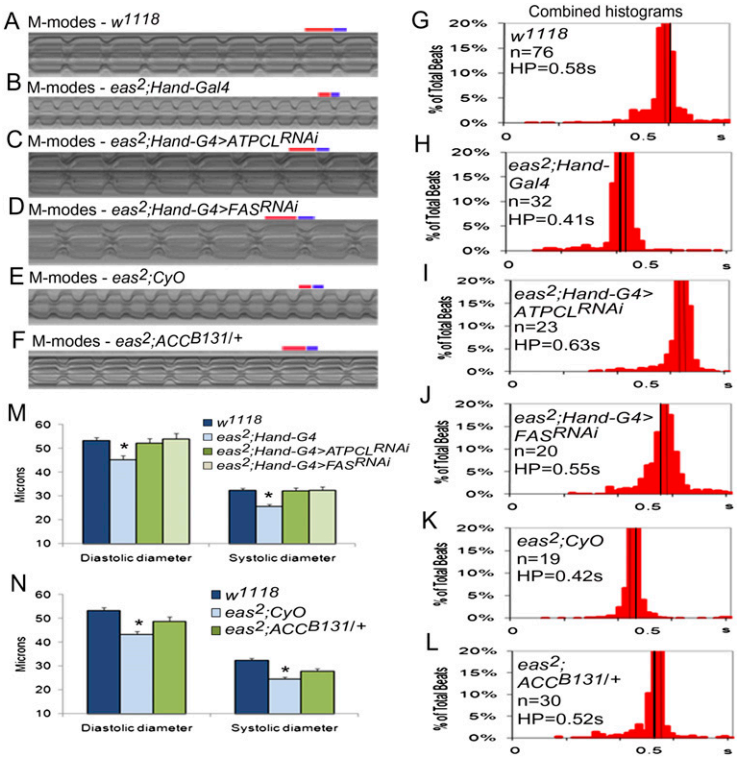

Figure 4. Dyslipidemia in *eas*^{2} flies is responsible for cardiac dysfunction. Combined HP histograms and M-mode traces (4.5-sec profiles) of 1-wk-old female hearts (*n* = number of hearts). Diastolic (red) and systolic (blue) intervals are indicated *above* each M-mode trace. Compared with wild-type (*w*^{1118}) (*A*,*G*), the outcrossed *eas*^{2} hearts (*B*,*E*,*H*,*K*) exhibit an obvious decrease in the HP, which is reinstated to normal levels upon the cardiac-specific down-regulation (*C*,*D*,*I*,*J*) or heterozygous loss (*F*,*L*) of genes that encode fatty acid biosynthetic enzymes. (*M*,*N*) Bar graph representations of changes in heart chamber dimensions. The diastolic and systolic diameters of 1-wk-old female outcrossed *eas*^{2} (light blue in *M*,*N*) hearts were significantly reduced relative to wild-type (*w*^{1118}, blue) hearts, but were significantly restored upon cardiac *RNAi* knockdown of *ATPCL* (green) or *FAS* (light green) (*M*) or elimination of one copy of *ACC* in the *eas*^{2} fly (green) (*N*). *P*-values ([*] $P < 0.05$) were calculated using the Student's *t*-test. Error bars indicate SEM.

firmly established. Our data show that the expression levels of ACC and FAS are up-regulated in flies harboring defects in PE synthesis (Fig. 3D–E) and may contribute to the observed cardiac derangements (Fig. 4; Supplemental Fig. S5). Both ACC and FAS were identified previously in tissue culture studies as being regulated by the dSREBP pathway (Dobrosotskaya et al. 2002; Seegmiller et al. 2002), suggesting that the dSREBP signaling pathway may be aberrant in these flies. Therefore, we tested the potential role of dSREBP in mediating the effects of an imbalance in PE metabolism on dyslipidemia and cardiac deficits in *eas*^{2} flies.

As a first step toward our goal, we determined whether dSREBP processing is altered in *eas*^{2} mutants. In wild-type flies (Fig. 5A, lane 1), endogenous dSREBP protein exists largely as a full-length, membrane-bound precursor (Fl-dSREBP), with small amounts detected as a cleaved, mature form (m-dSREBP). In contrast, *eas*^{2} flies display a greater proportion of m-dSREBP relative to the full-length protein (Fig. 5A, lane 2) than wild-type flies (Fig. 5A, lane 1). Similarly, flies with global RNAi-mediated *pect* and *cept* knockdown (*pect*^{i} and *cept*^{i}) also generate more m-dSREBP than controls (Fig. 5A, lanes 3–5). Thus, our in vivo data validate the in vitro observations that a disruption of PE biosynthesis induces the processing of dSREBP (Dobrosotskaya et al. 2002), leading most likely to compensatory hyperactivation of dSREBP signaling in response to constitutively low levels of PE in the *eas*^{2} fly .

We next examined how alterations of dSREBP activity could influence heart performance. No obvious effects on heart function were observed upon cardiac-specific inhibition of dSREBP activity in young unstressed flies (data not shown), which was achieved via the cardiac-specific overexpression of a dominant-negative form of dSREBP (*dSREBP*^{DN75T}) (Porstmann et al. 2008). However, the cardiac overexpression of a constitutively active form of dSREBP (m-dSREBP (Porstmann et al. 2008) and a full-length form of dSREBP (dSREBP^{FL}) (Porstmann et al. 2008) both led to a reduction in diastolic and systolic diameters as well as HP length relative to controls (Fig. 5B; Supplemental Fig. S6; Supplemental Table S2), reflecting the *eas*^{2} cardiac defects (Fig. 1E,G). Upon being subjected to pacing-induced stress, hearts that overexpress m-dSREBP underwent higher rates of failure compared with their respective controls at young ages (Fig. 5C), indicative of compromised cardiac performance, similar to *eas*^{2} hearts (Fig. 2A). Conversely, hearts that overexpress *dSREBP*^{DN75T} show significantly lower rates of stress-induced cardiac dysfunction at an older age relative to the control hearts (Fig. 5D), implying that the inhibition of *dSREBP* function augments cardiac resistance to stress at old age, which is reminiscent of the *Eas*$^+$-overexpressing hearts (Fig. 2C). These results, together with the increase in m-dSREBP protein in *eas*^{2} mutants (Fig. 5A), suggest that loss of *eas* and other perturbations resulting in PE deficiency triggers the elevated activation of dSREBP signaling, which is strongly associated with cardiac malfunction.

To test the above hypothesis further, we reduced dSREBP function in the *eas*^{2} mutant context to determine if the severity of cardiac anomalies is ameliorated. A global reduction of *dSREBP* expression in the *eas*^{2} fly was achieved by replacing one functional copy of *dSREBP* with its hypomorphic (*dSREBP*^{52}) counterpart (Kunte

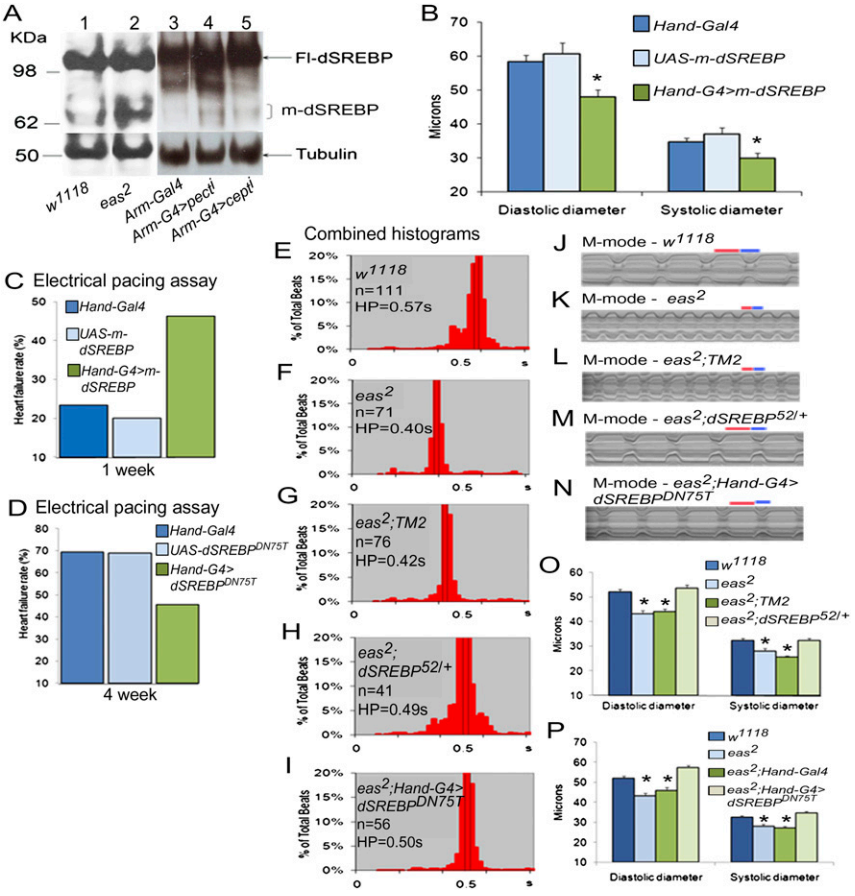

Figure 5. The dSREBP signaling pathway is aberrantly activated in the *eas*^{2} fly and contributes to its adiposity and cardiac abnormalities. (*A*) Immunoblot analysis of whole-fly lysates (50 μg of protein per lane) to reveal the full-length (Fl-dSREBP) and constitutively active, mature (m-dSREBP) forms of *Drosophila* SREBP protein. (*Bottom* panel) The same membrane was reprobed with anti-tubulin antibody as a loading control. (*Arm-G4>pectRNA*^{i}) The *RNAi* construct of *pect*; (*Arm-G4>ceptRNA*^{i}) the construct of *cept*^{i}. (*B*) Bar graph representations of cardiac chamber dimensions. Cardiac-specific overexpression of m-dSREBP results in significant reductions in both the diastolic and systolic dimensions of the heart chamber (green bars) in comparison with both the driver (blue) and transgene (light blue) controls. *P*-values ([⋆] $P < 0.05$) were calculated using the Student's *t*-test. Error bars indicate SEM. A similar trend was observed when overexpressing Fl-dSREBP (data not shown). (*C*,*D*) Genetic manipulations of dSREBP signaling and the effects on heart function under pacing-induced stress. (*C*) Cardiac overexpression of m-dSREBP results in young (1-wk-old) hearts being more susceptible to stress-induced failure relative to control groups (blue and light blue). (*D*) Cardiac overexpression of a dominant-negative form of dSREBP (dSREBP^{DN75T}) impeded the stress-induced decline in cardiac function in aged (4-wk-old) hearts. (*E–N*) Combined HP histograms and M-mode traces (2.5-sec traces) of pooled 1- and 3-wk-old female hearts (*n* = number of hearts). Diastolic (red) and systolic (blue) intervals are indicated *above* each M-mode trace. The evident decreases in the HPs of the *eas*^{2} (*F*,*K*) and outcrossed *eas*^{2} (*G*,*L*) hearts compared with wild-type hearts (*E*,*J*) were normalized upon the heterozygous loss of *dSREBP* (*H*,*M*) or heart expression of dominant-negative *dSREBP* (*dSREBP*^{DN75T}) in the *eas*^{2} background (*I*,*N*). (*O*,*P*) Bar graph representations of changes in heart chamber dimensions. The diastolic and systolic diameters of 1-wk-old female *eas*^{2} and outcrossed *eas*^{2} hearts (light blue and green, *O*,*P*) were significantly reduced relative to wild-type (*w*^{1118}) hearts (blue, *O*,*P*), but were significantly restored upon the heterozygous loss of *dSREBP* (light green, *O*) or heart expression of dominant-negative *dSREBP* (*dSREBP*^{DN75T}) (light green, *P*) in the *eas*^{2} background. *P*-values ([⋆] $P < 0.05$) were calculated using the Student's *t*-test. Error bars indicate SEM.

et al. 2006), and this is sufficient to restore the lengthened HP of *eas*^{2} flies to normal durations (Fig. 5F–H,K–M). Moreover, the constricted heart diameters of *eas*^{2} flies were restored to wild-type levels in *eas*^{2} flies harboring *dSREBP*^{52} heterozygosis (Fig. 5O; Supplemental Table S1). Similar rescues of *eas*^{2} cardiac defects were achieved with a null allele of *dSREBP* (*dSREBP*^{189}) (Kunte et al. 2006) in the *eas*^{2} background (Supplemental Fig. S7; Supplemental Table S1). To further examine if up-regulation of dSREBP signaling contributes to the *eas* cardiac defects in a tissue-autonomous manner, we genetically suppressed the activity of dSREBP specifically in *eas*^{2} hearts by cardiac-specific expression of *dSREBP*^{DN75T} in *eas*^{2} mutants (Fig. 5; Supplemental Table S1). There is a significant restoration of both the faster heart rate and heart tube dimensions in those transgenic flies (Fig. 5I,N,P). Finally, the improved cardiac parameters in *eas*^{2} flies harboring reduced dSREBP expression (*dSREBP*^{52}) or activity (dSREBP^{DN75T}) are paralleled by a decrease in overall and cardiac accumulation of TG (Fig. 3A,B). Taken together, these results demonstrate that the compensatory hyperactivation of dSREBP signaling in the *eas*^{2} flies plays a causative role in inducing deterioration of heart function by generating a state of dyslipidemia.

eas^2 *hearts and hearts overexpressing m-dSREBP exhibit structural defects*

To further determine whether increased dSREBP signaling and lipogenesis in the *eas*^{2} fly adversely affects the cytoarchitecture of the myocyte, we visualized myofibrils in the adult heartthat include densely packed transverse myofibrils in the myocardium and a layer of longitudinal muscle fibers associated with the ventral surface of the heart (Molina and Cripps 2001). Compared with the wild type, the *eas*^{2} hearts displayed severe degeneration and disorganization of the longitudinal and, to a lesser extent, inner transverse myofibrils (Figs.

1H,H′, 6A–B′). The expression of wild-type *Eas*$^{+}$ cDNA, *dSREBP*^{DN75T}, and *fas*^{RNAi} (Fig. 6C–E′) in the *eas*^{2} heart results in robust restoration of myofibrillar integrity, which includes the re-establishment of longitudinal myofibrils (Fig. 6C,D,E, arrows). Of note, we were able to achieve substantial rescue of the *eas*^{2} longitudinal myofibrils upon the expression of these constructs using *Hand-Gal4*, as this driver appears to be active only in the cardiomyocytes containing transverse myofibrils (see the Materials and Methods). Moreover, overexpression of *m-dSREBP* (activated form) in the heart using *Hand-Gal4* phenocopies the *eas*^{2} mutation in the myocardium and causes significant loss of longitudinal fibers and disarrayed inner transverse myofibrils, compared with control hearts (Fig. 6F–G′). Taken together, these observations suggest that the structural alterations in the *eas*^{2} hearts, like the functional deficits, are a consequence of a defect in PE homeostasis and elevation in dSREBP pathway and

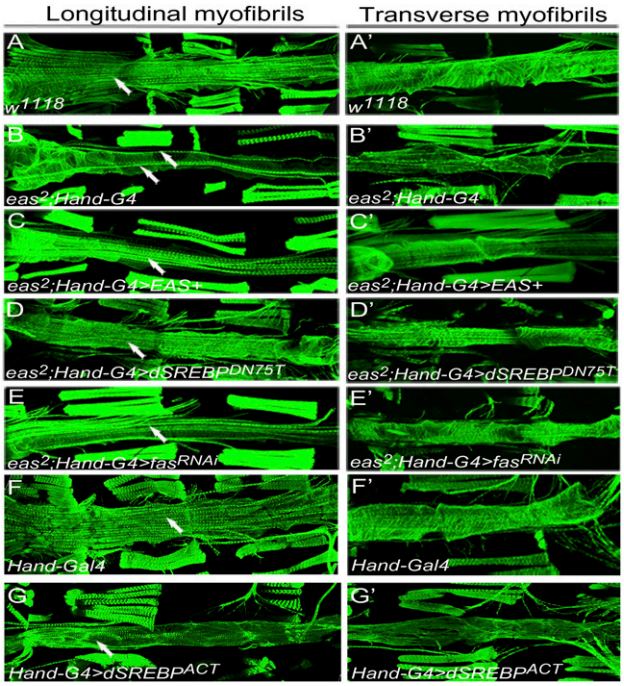

Figure 6. One-week-old *eas*^{2} hearts and hearts overexpressing m-dSREBP exhibit structural defects. Representative confocal stacks of hearts (anterior to left) stained with actin-phalloidin (green). (*A–E′*) Compared with wild-type (*w*^{1118}) hearts (*A,A′*), the outcrossed *eas*^{2}*;Hand-G4* hearts show significant sarcomeric disorganization of the longitudinal fibers, as indicated by the fewer longitudinal fibers (arrows in *B*). (*B′*) Cardiac spiral myofibers appear to undergo degeneration to a certain extent. (*C–E′*) The *eas*^{2} hearts overexpressing a wild-type *Eas*$^{+}$ construct (*C,C′*), dominant-negative *dSREBP* (*dSREBP*^{DN75T}) (*D,D′*), or an *RNAi* construct against FAS (*fas*^{RNAi}) (*E,E′*) appear to regain near-normal amounts of cardiac longitudinal myofibrils (arrows, *C,D,E*) and proper organization of transverse myofibrils. (*F,F′*) *Hand-Gal4* driver control hearts showing well-organized ventral longitudinal myofibrils (arrows in *F*) and inner transverse myofibrils (*F′*). (*G,G′*) *Hand-G4* driving m-dSREBP hearts showing significant loss of longitudinal myofibrils (arrows in *G*) and disorganized transverse myofibrils (*G′*).

lipid synthesis. In addition, the genetic manipulations of cardiomyocytes may have significant non-cell-autonomous effects on the ventral muscle layer containing the longitudinal myofibrils. These longitudinal muscles are closely associated with the heart tube, and have been proposed to assist in circulation of the hemolymph through the heart tube (Molina and Cripps 2001). It is therefore possible that the disposition of the cardiomyocytes influences the integrity of the longitudinal muscles such that abnormalities in them contribute to cardiac dysfunction in the *eas*^{2} mutants. This interpretation is corroborated by previous studies in which genetic manipulations with cardiomyocyte-specific drivers also affect these longitudinal muscles (Birse et al. 2010; Neely et al. 2010). In obese and diabetic rodent models and human subjects, myocardial steatosis correlates with functional and structural changes of the heart (Abel et al. 2008; Harmancey et al. 2008), which is consistent with our findings of *eas*^{2} mutants. It has also been implicated that diabetes-induced changes in membrane phospholipid content and hydrolysis may contribute to some of the alterations in myocardial function that are observed in diabetic patients (McHowat et al. 2000; Su et al. 2005). *Drosophila eas* could potentially serve as a useful model for exploring the cardiac effects of metabolic syndrome and type 2 diabetes.

Discussion

In this study, we used *Drosophila* genetic approaches to identify a novel metabolic cardiomyopathy that exhibits striking features of obesity- and diabetes-related heart failure in humans. Specifically, we showed that a genetically dysregulated phospholipid metabolism leads to chronic stimulation of the transcription factor dSREBP and its lipogenic target genes, which in turn leads to cardiac fat accumulation associated with electrical and functional signatures of heart failure. This study highlights a regulatory relationship between the PE phospholipid and TG metabolism that could play a major role in eliciting cardiac steatosis and dysfunction, and identifies the dSREBP signaling pathway as the key metabolic pathway that underlies the increased synthesis and accumulation of TG upon the disruption of PE homeostasis.

Our current data led us to put forth a model (Fig. 7) that describes how the dysregulation of membrane PE homeostasis could promote the pathogenesis of lipotoxic cardiomyopathy. In wild-type flies, a decrease in membrane PE level triggers the proteolytic release of a transcriptionally active form of dSREBP (m-dSREBP) and induces the biosynthesis of fatty acids in a manner similar to that in mammals (Nohturfft and Losick 2002; see also above). Upon the subsequent use of these fatty acids in PE synthesis, and the restoration of normal PE concentrations in cellular membranes, further processing of dSREBP is blocked and overall lipid synthesis is reduced. The presence of such a feedback inhibitory loop ensures that PE homeostasis can be achieved under physiological conditions. In flies harboring a genetic perturbation of the CDP–ethanolamine pathway, the failure to produce PE and the

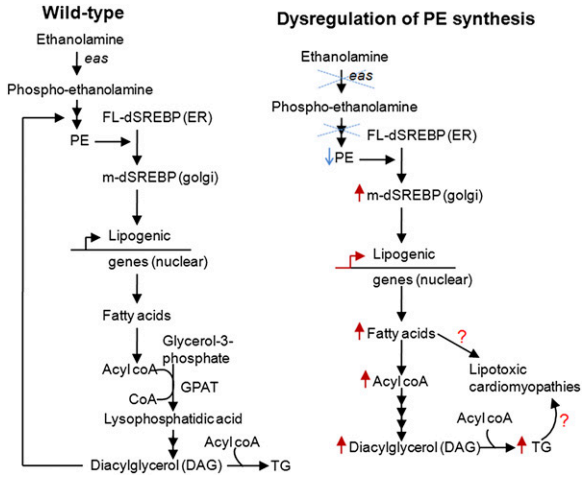

Figure 7. A model depicting how the dysregulation of PE homeostasis may give rise to cardiac impairments in the *eas*^{2} fly. PE level is maintained in wild-type flies (w^{1118}) via dSREBP sensing and activation. The perturbation of PE homeostasis (blue crosses) and constitutively reduced level of PE (blue arrow) in the *eas* fly induces constant compensatory overactivation (red arrows) of dSREBP signaling and excessive lipid production, resulting in lipotoxic cardiomyopathy.

ensuing low levels of PE disrupt the homeostatic negative feedback loop, resulting in the continuous activation of the dSREBP pathway. Prolonged stimulation of lipogenesis and the oversupply of lipid intermediates such as acyl coA and DAG could lead to increased production of TG, resulting in hypertriglyceridemia, cardiac steatosis, and the progressive development of lipotoxic cardiomyopathy.

It is possible that the above phenomenon, although identified in a fly model, also occurs in mammals. In fact, in mice, elimination of the CDP–ethanolamine pathway resulting in the absence of PE synthesis induced a significant elevation of TG levels (Fullerton et al. 2009; Leonardi et al. 2009). Along with hypertriglyceridemia, it was also observed in these studies that the expression of key fatty acid biosynthetic genes such as *ACC* and *FAS* is up-regulated in PE-deficient mice. It has been proposed that the elevated TG concentration is due to an increased availability of DAG arising from its underutilization by the CDP–ethanolamine pathway that leads to a redirection of DAG to TG formation (see Fig. 7; Fullerton et al. 2009; Leonardi et al. 2009). However, this proposal fails to explain how the passive accumulation of DAG in the PE-deprived state could induce an upstream event such as the expression of the lipogenic genes (see Fig. 7). The mechanism proposed in our model based on the *eas*^{2} fly studies could reconcile to some extent this dilemma in the mammalian system. Our model posits that constitutively low levels of PE drive a compensatory hyperactivation of the SREBP pathway. Once activated, SREBP can induce de novo lipogenesis and the active generation of intermediates such as acyl coA and DAG, a sequence of steps that culminates in the heightened production of TG (Fig. 7). Indeed, in mice lacking the capacity to generate PE, the expression of one of the mammalian SREBP isoforms, *SREBP-1c*, was found to be up-regulated (Fullerton et al. 2009; Leonardi et al. 2009). Furthermore, the PE-deficient mice also develop metabolic disorders such as hepatic steatosis and insulin resistance (Fullerton et al. 2009; Leonardi et al. 2009). However, it remains to be seen whether SREBP signaling might similarly be regulated by PE homeostasis in mammals such that a deficit in PE levels elicits an activation of the SREBP pathway to generate increased amounts of fatty acids and DAG/TG. It would be interesting to test whether the enhanced levels of TGs, as well as the severity of these phenotypes, would be significantly ameliorated upon the down-regulation of *SREBP* expression or activity in these mice, indicating a primary role of SREBP signaling in mediating the development of hypertriglyceridemia and its related metabolic disorders upon the perturbation of PE synthesis in the mammalian context.

Concluding remarks

Our model, based on studies in *Drosophila eas* mutants, provides insights into the potential role of the dSREBP signaling pathway in coupling membrane phospholipid homeostasis with lipid metabolism and its associated metabolic functions. Our findings also support the notion that *Drosophila* shares many of the basic metabolic functions found in vertebrates (Baker and Thummel 2007), and that the genetic dissection of the metabolic and transcriptional responses in a less complex model organism such as *Drosophila* facilitates our understanding of fundamental aspects of metabolic control, cardiac physiology, and associated disease mechanisms.

Materials and methods

Fly stocks

Drosophila strains were maintained on standard cornmeal–molasses agar medium at room temperature (22°C–25°C). The *eas* gene is located at 14B on the cytological map and encodes an ethanolamine kinase (Pavlidis et al. 1994). The *eas* allele used in this study is *eas*^{2} (also known as *eas*^{PC80}), provided by M. Tanouye (University of California at Berkeley). It is caused by a 2-base-pair (bp) deletion that introduces a frame shift; the resulting truncated protein lacks a kinase domain and abolishes all enzymatic activity. The w^{1118}, *eas*^{alaP} allele was induced by *P(GawB)* mutagenesis (Boquet et al. 2000), and was obtained from Thomas Preat (CNRS, France). The *eas*^{KG01772}, *ACC*^{B131}, and *FAS*^{KG3696} alleles were received from the Bloomington Stock Center. The myocardial-specific GAL4 drivers were *Hand-Gal4* (generous gift from L. Perrin). Hand-Gal4 was found to be expressed in myocardial cells but not in the muscle cells containing the longitudinal fibers. This is in agreement what was reported previously by Han et al. (2006) and Togel et al. (2008) for Hand-Gal4 constructs. *GMH5* was described previously (Wessells et al. 2004). *UAS-pect*^{RNAi}, *UAS-cept*^{RNAi}, *UAS-ACC*^{RNAi}, *UAS-ATPCL*^{RNAi}, *UAS-FAS*^{RNAi}, and *UAS-GFP* were from the Vienna *Drosophila* RNAi Center and Bloomington Stock Center. *UAS-Eas*$^{+}$ (Pascual et al. 2005) was received from Thomas Preat (CNRS, France). The dSREBP fly stocks (UAS-dSREBP^{DN}, UAS-m-dSREBP, dSREBP^{52}, and dSREBP^{189} alleles) were kindly provided by Robert B. Rawson (University of Texas Southwestern Medical Center, Dallas).

Antibodies

Anti-EAS (Pascual et al. 2005) (a gift from Thomas Preat) and anti-α-tubulin (B-5-1-2, Sigma) were used for immunoblot analyses. The anti-human IgG-2A4 SREBP-1 antibody was purchased from BD Biosciences, and was used at 1:1000 for immunoblotting. This monoclonal antibody was raised against amino acid residues 301–407 in human SREBP-1a and has been shown previously to cross-react with dSREBP (Theopold et al. 1996; Rosenfeld and Osborne 1998). The anti-human ACC antibody (#3662) and anti-human ATPCL antibody (#4332) were purchased from Cell Signaling Technology, Inc.. The cross-reactivities of these human antibodies against *Drosophila* ACC and ATPCL proteins were determined by the following: First, immunoblot analysis of wild-type fly lysates using these two antibodies revealed bands that correspond to the predicted sizes of *Drosophila* ACC and ATPCL proteins (Supplemental Fig. S4). Second, immunoblot analysis of the $ACC^{B131/+}$ fly lysate using the anti-human ACC antibody revealed a significant diminution of the predicted ACC band, as did the predicted ATPCL band upon immunoblot analysis of the $ATPCL^{23402}$ fly lysates using anti-human ATPCL antibody (Supplemental Fig. S4). Note that the ATPCL band in the w^{1118} lane in Figure S4A has been subjected to longer exposure than the ATPCL band in the w^{1118} lane in Figure 3D′. Third, the anti-human ACC antibody is predicted to cross-react with *Drosophila* ACC based on 100% sequence homology with the residues surrounding Lys 557 of human ACCα1 (Cell Signaling, #3662 product sheet). For immunostaining purposes, fluorescein-labeled phalloidin (Invitrogen) and mouse anti-actinin (Saide et al. 1989) were used.

Immunostaining

Adult female flies (7–10 d old) were dissected to expose the heart and were fixed for 15 min in 4% paraformaldehyde. After washing in PBS plus 0.1% Triton X-100 (PBT-0.1), the fixed hearts were incubated overnight at 4°C with primary antibodies appropriately diluted in PBT-0.1. The tissues were then washed with PBT-0.1 and incubated with fluorescence-conjugated secondary antibodies. The following antibodies were used at the concentrations indicated: mouse anti-α-actinin (1:20) and fluorescein-labeled phalloidin (1:20). Secondary antibodies were FITC-conjugated anti-mouse and Cy3-conjugated anti-rabbit IgG (Sigma). Samples were mounted in VectaShield (Vector Laboratories). Images were acquired on an MRC 1024 SP Bio-Rad laser point scanning confocal microscope using LaserSharp 2000 software (Bio-Rad). Consecutive confocal sections were acquired in the *Z*-axis with a step of 2 μm and were projected in ImageJ software.

Immunoblotting

For whole adult protein analysis of Eas, ACC, and ATPCL, 7- to 10-d-old female flies were homogenized in cell lysis buffer (PBT-0.1) supplemented with a cocktail of protease inhibitors. For whole adult protein analysis of dSREBP, flies were homogenized in buffer F (125 mM Tris-HCl at pH 6.8, 8 M urea, 5% SDS) supplemented with a cocktail of protease inhibitors (Matthews et al. 2010). Lysates were clarified by centrifugation, boiled in 1× SDS sample buffer, resolved by SDS-PAGE, transferred onto PVDF membranes, and probed with the relevant antibodies as described above. Chemiluminescence was detected using ECL Plus Western blotting detection reagents (Amersham).

TG measurement

For quantification of TGs in whole flies, crude lysates of 10 adult female flies (7–10 d old) in lysis buffer PBT-0.05 (PBS plus 0.05% Triton X-100) were prepared by homogenization or sonication. For quantification of TGs in hearts, 20–25 adult female hearts (7–10 d old) were lysed in PBT by brief sonication. TG amounts were measured using Infinity Triglycerides assay kit (Thermo Electron Scientific, catalog no. TR22421) according to manufacturer's instructions, and were normalized to protein amounts measured by the Bio-Rad protein assay kit (Bio-Rad).

Fly heartbeat analysis

To measure cardiac function parameters, a semi-intact preparation of fly heart was analyzed according to previously described protocols (K Ocorr et al. 2007a,b; Ocorr et al. 2009). High-speed 30- to 60-sec movies were taken at a rate of >100 frames per second using a Hamamatsu CCD camera on a Leica DM LFSA microscope with a 10× dipping immersion lens. The images were processed using Simple PCI imaging software (Compix, Inc.). M-modes and quantitative data were generated using a MatLab-based image analysis program (K Ocorr et al. 2007a,b; Ocorr et al. 2009). Briefly, to generate M-mode figures, a single-pixel-wide column that encompasses both edges of the heart tube was selected, and corresponding columns were cut from all movie frames and aligned horizontally according to time. Thus, the M-mode provides an edge trace that documents the movement of the heart tube walls in the *Y*-axis over time in the *X*-axis. HPs are defined as the time between the ends of two consecutive diastolic intervals. Diastolic interval is the time taken for the heart to relax, and systolic interval is the time taken for the heart to contract. Diastolic diameter is the diameter of the opposing heart wall during a period of relaxation; systolic diameter is the diameter of the opposing heart wall during a period of constriction. Measurements for the diastolic and systolic diameters were taken from the most posterior portion of the heart at the abdominal A3 segment (region of the valve). Only female hearts were analyzed in this study.

Electrical pacing

To measure adult heart response to external electrical pacing, intact fly hearts were analyzed according to previously described protocols (Wessells et al. 2004, 2009; KA Ocorr et al. 2007). Briefly, eight to 10 female flies were placed between two electrodes touching conductive jelly spread over the electrodes. Their hearts were paced with a square wave stimulator at 40 V and 6 Hz for 30 sec. Hearts were visually scored between 60 and 90 sec after pacing for signs of arrest or fibrillation. Heart failure rate is defined as the percentage of flies that enter either cardiac arrest or fibrillation.

Acknowledgments

We thank Mark Tanouye, Rob Rawson, and Thomas Preat for reagents and fly stocks. We also thank Daniel Kelly, Timothy Osborne, and Michael Karin for critical reading of an earlier version of the manuscript, and Tom Kornberg, Yuh-Nung Jan, and Takashi Mikawa for their helpful suggestions. We thank Lisa Elmén for technical assistance and fly stock curating. H.Y.L is supported by a post-doctoral fellowship (Western Affiliate) of the American Heart Association (AHA). K.O. is supported by a Scientist Development Grant of the American Heart Association (AHA). R.B. is supported by grants from NHLBI of the National Institutes of Health, the Muscular Dystrophy Association, and the Ellison Medical Foundation.

References

Abel ED, Litwin SE, Sweeney G. 2008. Cardiac remodeling in obesity. *Physiol Rev* **88:** 389–419.

Baker KD, Thummel CS. 2007. Diabetic larvae and obese flies-emerging studies of metabolism in *Drosophila*. *Cell Metab* **6:** 257–266.

Birse RT, Choi J, Reardon K, Rodriguez J, Graham S, Diop S, Ocorr K, Bodmer R, Oldham S. 2010. High-fat-diet-induced obesity and heart dysfunction are regulated by the TOR pathway in *Drosophila*. *Cell Metab* **12:** 533–544.

Boquet I, Hitier R, Dumas M, Chaminade M, Preat T. 2000. Central brain postembryonic development in *Drosophila*: Implication of genes expressed at the interhemispheric junction. *J Neurobiol* **42:** 33–48.

Bugger H, Abel ED. 2008. Molecular mechanisms for myocardial mitochondrial dysfunction in the metabolic syndrome. *Clin Sci (Lond)* **114:** 195–210.

Caviglia JM, De Gomez Dumm IN, Coleman RA, Igal RA. 2004. Phosphatidylcholine deficiency upregulates enzymes of triacylglycerol metabolism in CHO cells. *J Lipid Res* **45:** 1500–1509.

Chiu HC, Kovacs A, Ford DA, Hsu FF, Garcia R, Herrero P, Saffitz JE, Schaffer JE. 2001. A novel mouse model of lipotoxic cardiomyopathy. *J Clin Invest* **107:** 813–822.

Chiu HC, Kovacs A, Blanton RM, Han X, Courtois M, Weinheimer CJ, Yamada KA, Brunet S, Xu H, Nerbonne JM, et al. 2005. Transgenic expression of fatty acid transport protein 1 in the heart causes lipotoxic cardiomyopathy. *Circ Res* **96:** 225–233.

Christoffersen C, Bollano E, Lindegaard ML, Bartels ED, Goetze JP, Andersen CB, Nielsen LB. 2003. Cardiac lipid accumulation associated with diastolic dysfunction in obese mice. *Endocrinology* **144:** 3483–3490.

Dobrosotskaya IY, Seegmiller AC, Brown MS, Goldstein JL, Rawson RB. 2002. Regulation of SREBP processing and membrane lipid production by phospholipids in *Drosophila*. *Science* **296:** 879–883.

Fast PG. 1966. A comparative study of the phospholipids and fatty acids of some insects. *Lipids* **1:** 209–215.

Fink M, Callol-Massot C, Chu A, Ruiz-Lozano P, Izpisua Belmonte JC, Giles W, Bodmer R, Ocorr K. 2009. A new method for detection and quantification of heartbeat parameters in *Drosophila*, zebrafish, and embryonic mouse hearts. *Biotechniques* **46:** 101–113.

Fullerton MD, Hakimuddin F, Bonen A, Bakovic M. 2009. The development of a metabolic disease phenotype in CTP:phosphoethanolamine cytidylyltransferase-deficient mice. *J Biol Chem* **284:** 25704–25713.

Han Z, Yi P, Li X, Olson EN. 2006. Hand, an evolutionarily conserved bHLH transcription factor required for *Drosophila* cardiogenesis and hematopoiesis. *Development* **133:** 1175–1182.

Harmancey R, Wilson CR, Taegtmeyer H. 2008. Adaptation and maladaptation of the heart in obesity. *Hypertension* **52:** 181–187.

Janero DR, Burghardt C, Feldman D. 1988. Amphiphile-induced heart muscle-cell (myocyte) injury: Effects of intracellular fatty acid overload. *J Cell Physiol* **137:** 1–13.

Kennedy EP. 1957. Metabolism of lipides. *Annu Rev Biochem* **26:** 119–148.

Kunte AS, Matthews KA, Rawson RB. 2006. Fatty acid auxotrophy in *Drosophila* larvae lacking SREBP. *Cell Metab* **3:** 439–448.

Leonardi R, Frank MW, Jackson PD, Rock CO, Jackowski S. 2009. Elimination of the CDP–ethanolamine pathway disrupts hepatic lipid homeostasis. *J Biol Chem* **284:** 27077–27089.

Matthews KA, Ozdemir C, Rawson RB. 2010. Activation of SREBP in the absence of Scap in *Drosophila melanogaster*. *Genetics* **185:** 189–198.

McHowat J, Creer MH, Hicks KK, Jones JH, McCrory R, Kennedy RH. 2000. Induction of Ca-independent PLA(2) and conservation of plasmalogen polyunsaturated fatty acids in diabetic heart. *Am J Physiol Endocrinol Metab* **279:** E25–E32.

McMaster CR, Choy PC. 1992. Serine regulates phosphatidylethanolamine biosynthesis in the hamster heart. *J Biol Chem* **267:** 14586–14591.

Molina MR, Cripps RM. 2001. Ostia, the inflow tracts of the *Drosophila* heart, develop from a genetically distinct subset of cardial cells. *Mech Dev* **109:** 51–59.

Neely GG, Kuba K, Cammarato A, Isobe K, Amann S, Zhang L, Murata M, Elmen L, Gupta V, Arora S, et al. 2010. A global in vivo *Drosophila* RNAi screen identifies NOT3 as a conserved regulator of heart function. *Cell* **141:** 142–153.

Nohturfft A, Losick R. 2002. Cell biology. Fats, flies, and palmitate. *Science* **296:** 857–858.

Nyako M, Marks C, Sherma J, Reynolds ER. 2001. Tissue-specific and developmental effects of the easily shocked mutation on ethanolamine kinase activity and phospholipid composition in *Drosophila melanogaster*. *Biochem Genet* **39:** 339–349.

Ocorr K, Perrin L, Lim HY, Qian L, Wu X, Bodmer R. 2007a. Genetic control of heart function and aging in *Drosophila*. *Trends Cardiovasc Med* **17:** 177–182.

Ocorr K, Reeves NL, Wessells RJ, Fink M, Chen HS, Akasaka T, Yasuda S, Metzger JM, Giles W, Posakony JW, et al. 2007b. KCNQ potassium channel mutations cause cardiac arrhythmias in *Drosophila* that mimic the effects of aging. *Proc Natl Acad Sci* **104:** 3943–3948.

Ocorr KA, Crawley T, Gibson G, Bodmer R. 2007. Genetic variation for cardiac dysfunction in *Drosophila*. *PLoS ONE* **2:** e601. doi: 10.1371/journal.pone.0000601.

Ocorr K, Fink M, Cammarato A, Bernstein S, Bodmer R. 2009. Semi-automated optical heartbeat analysis of small hearts. *J Vis Exp* **31**. http://www.jove.com/index/details.stp?id=1435. doi: 10.3791/1435.

Osborne TF, Espenshade PJ. 2009. Evolutionary conservation and adaptation in the mechanism that regulates SREBP action: What a long, strange tRIP it's been. *Genes Dev* **23:** 2578–2591.

Ostrander DB, Sparagna GC, Amoscato AA, McMillin JB, Dowhan W. 2001. Decreased cardiolipin synthesis corresponds with cytochrome *c* release in palmitate-induced cardiomyocyte apoptosis. *J Biol Chem* **276:** 38061–38067.

Pascual A, Chaminade M, Preat T. 2005. Ethanolamine kinase controls neuroblast divisions in *Drosophila* mushroom bodies. *Dev Biol* **280:** 177–186.

Pavlidis P, Ramaswami M, Tanouye MA. 1994. The *Drosophila* easily shocked gene: A mutation in a phospholipid synthetic pathway causes seizure, neuronal failure, and paralysis. *Cell* **79:** 23–33.

Porstmann T, Santos CR, Griffiths B, Cully M, Wu M, Leevers S, Griffiths JR, Chung YL, Schulze A. 2008. SREBP activity is regulated by mTORC1 and contributes to Akt-dependent cell growth. *Cell Metab* **8:** 224–236.

Post JA, Bijvelt JJ, Verkleij AJ. 1995. Phosphatidylethanolamine and sarcolemmal damage during ischemia or metabolic inhibition of heart myocytes. *Am J Physiol* **268:** H773–H780.

Rosenfeld JM, Osborne TF. 1998. HLH106, a *Drosophila* sterol regulatory element-binding protein in a natural cholesterol auxotroph. *J Biol Chem* **273:** 16112–16121.

Saide JD, Chin-Bow S, Hogan-Sheldon J, Busquets-Turner L, Vigoreaux JO, Valgeirsdottir K, Pardue ML. 1989. Characterization of components of Z-bands in the fibrillar flight muscle of *Drosophila melanogaster*. *J Cell Biol* **109:** 2157–2167.

Schulze PC. 2009. Myocardial lipid accumulation and lipotoxicity in heart failure. *J Lipid Res* **50:** 2137–2138.

Seegmiller AC, Dobrosotskaya I, Goldstein JL, Ho YK, Brown MS, Rawson RB. 2002. The SREBP pathway in *Drosophila*: Regulation by palmitate, not sterols. *Dev Cell* **2:** 229–238.

Sentex E, Sergiel JP, Lucien A, Grynberg A. 1997. Trimetazidine increases phospholipid turnover in ventricular myocyte. *Mol Cell Biochem* **175:** 153–162.

Sentex E, Sergiel JP, Lucien A, Grynberg A. 1998. Is the cytoprotective effect of trimetazidine associated with lipid metabolism? *Am J Cardiol* **82:** 18K–24K. doi: 10.1016/S0002-9149(98)00533-5.

Shimano H. 2009. SREBPs: Physiology and pathophysiology of the SREBP family. *FEBS J* **276:** 616–621.

Son NH, Park TS, Yamashita H, Yokoyama M, Huggins LA, Okajima K, Homma S, Szabolcs MJ, Huang LS, Goldberg IJ. 2007. Cardiomyocyte expression of PPARγ leads to cardiac dysfunction in mice. *J Clin Invest* **117:** 2791–2801.

Su X, Han X, Mancuso DJ, Abendschein DR, Gross RW. 2005. Accumulation of long-chain acylcarnitine and 3-hydroxy acylcarnitine molecular species in diabetic myocardium: Identification of alterations in mitochondrial fatty acid processing in diabetic myocardium by shotgun lipidomics. *Biochemistry* **44:** 5234–5245.

Tabbi-Anneni I, Helies-Toussaint C, Morin D, Bescond-Jacquet A, Lucien A, Grynberg A. 2003. Prevention of heart failure in rats by trimetazidine treatment: A consequence of accelerated phospholipid turnover? *J Pharmacol Exp Ther* **304:** 1003–1009.

Tappia PS, Singal T. 2008. Phospholipid-mediated signaling and heart disease. *Subcell Biochem* **49:** 299–324.

Theopold U, Ekengren S, Hultmark D. 1996. HLH106, a *Drosophila* transcription factor with similarity to the vertebrate sterol responsive element binding protein. *Proc Natl Acad Sci* **93:** 1195–1199.

Togel M, Pass G, Paululat A. 2008. The *Drosophila* wing hearts originate from pericardial cells and are essential for wing maturation. *Dev Biol* **318:** 29–37.

Unger RH, Orci L. 2002. Lipoapoptosis: Its mechanism and its diseases. *Biochim Biophys Acta* **1585:** 202–212.

Vance JE. 2008. Phosphatidylserine and phosphatidylethanolamine in mammalian cells: Two metabolically related aminophospholipids. *J Lipid Res* **49:** 1377–1387.

Vecchini A, Del Rosso F, Binaglia L, Dhalla NS, Panagia V. 2000. Molecular defects in sarcolemmal glycerophospholipid subclasses in diabetic cardiomyopathy. *J Mol Cell Cardiol* **32:** 1061–1074.

Wessells RJ, Bodmer R. 2004. Screening assays for heart function mutants in *Drosophila*. *Biotechniques* **37:** 58–66.

Wessells RJ, Fitzgerald E, Cypser JR, Tatar M, Bodmer R. 2004. Insulin regulation of heart function in aging fruit flies. *Nat Genet* **36:** 1275–1281.

Wessells R, Fitzgerald E, Piazza N, Ocorr K, Morley S, Davies C, Lim HY, Elmen L, Hayes M, Oldham S, et al. 2009. d4eBP acts downstream of both dTOR and dFoxo to modulate cardiac functional aging in *Drosophila*. *Aging Cell* **8:** 542–552.

Yagyu H, Chen G, Yokoyama M, Hirata K, Augustus A, Kako Y, Seo T, Hu Y, Lutz EP, Merkel M, et al. 2003. Lipoprotein lipase (LpL) on the surface of cardiomyocytes increases lipid uptake and produces a cardiomyopathy. *J Clin Invest* **111:** 419–426.

Yang R, Barouch LA. 2007. Leptin signaling and obesity: Cardiovascular consequences. *Circ Res* **101:** 545–559.

Yao Y, Huang C, Li ZF, Wang AY, Liu LY, Zhao XG, Luo Y, Ni L, Zhang WG, Song TS. 2009. Exogenous phosphatidylethanolamine induces apoptosis of human hepatoma HepG2 cells via the bcl-2/Bax pathway. *World J Gastroenterol* **15:** 1751–1758.

Phospholipid homeostasis regulates lipid metabolism and cardiac function through SREBP signaling in *Drosophila*

Hui-Ying Lim, Weidong Wang, Robert J. Wessells, et al.

Genes Dev. 2011, **25:**
Access the most recent version at doi:10.1101/gad.1992411